Available online at www.sciencedirect.com

ScienceDirect

Ceramics International 40 (2014) 4791–4795

CERAMICS INTERNATIONAL

www.elsevier.com/locate/ceramint

Single-microemulsion-based solvothermal synthesis of magnetite microflowers

Yanfen Li, Rongli Jiang*, Tingyu Liu, Hui Lv, Xiaoyu Zhang

School of Chemical Engineering and Technology, China University of Mining and Technology, Xuzhou 221116, PR China

Received 12 July 2013; received in revised form 6 September 2013; accepted 7 September 2013
Available online 16 September 2013

Abstract

Flower-like magnetite (Fe_3O_4) microstructures have been successfully prepared through a novel single-microemulsion-mediated solvothermal route at a relatively low temperature. X-ray diffraction (XRD), field-emission scanning electron microscopy (FE-SEM) and transmission electron microscopy (TEM) were employed to characterize the samples. The time-dependent experiments were conducted to explore the growth mechanism. Room temperature magnetic measurement reveals that the as-obtained Fe_3O_4 flower-like structures possess a high saturation magnetization and exhibit a superparamagnetic nature, making them potentially useful in environmental and biomedical applications.

Keywords: C. Magnetic properties; Magnetite; Flower-like structures; Growth from solutions

1. Introduction

In the past decades, iron oxides have received much attention because of their low cost, abundance, and environmental friendliness [1,2]. Fe_3O_4 is one of the most important crystal phases among iron oxides. It is a kind of significant magnetic material with the bulk saturation magnetization of about 85–100 emu/g [3]. Micro/nanostructured Fe_3O_4 is of great importance in various fields, including biomaterials diagnostics, catalysis, ferrofluids, magnetic resonance imaging, immunoassay, drug and gene delivery [4–7]. To date, a series of solution-based routes and vapor-phase process have been developed for the synthesis of Fe_3O_4. Numerous Fe_3O_4 micro/nanostructures, such as nanoparticles [8], one-dimensional (1D) nanorods [9,10], nanowires [11], nanotubes [12], nanobelts [13], nanochains [14], two-dimensional (2D) nanosheets [15], three-dimensional (3D) dendrite-like [16], dandelion-like [17], wafer-like [18] nanostructures have been fabricated by these strategies. However, to the best of our knowledge, there are only limited publications on the preparation of hierarchical Fe_3O_4 flower-like micro/nanostructures, which have high specific surface areas are the most suitable candidates for sensors and wastewater treatment. For example, flower-shaped Fe_3O_4 structures prepared through an ethylene-glycol-mediated self-assembly process demonstrated excellent ability to remove various pollutants from water [19]. Fe_3O_4 flower-like structures formed by a microwave-assisted ethylene glycol approach in the presence of the PEO-PPO-PEO block copolymers displayed attractive magnetic and gas sensing properties [20]. Hierarchical Fe_3O_4 flower-like structures obtained via an ultrasound-assisted hydrothermal route and subsequent calcining process exhibited a strong capability to get rid of organic contaminants [21].

Although much progress has been made in synthesis of hierarchical magnetite architectures, mild synthetic routes under moderate temperature are still required. Herein, we report a novel and facile single-microemulsion-based solvothermal method to fabricate Fe_3O_4 micrometer-scale crystals with flower-like morphologies. The Fe_3O_4 microflowers can be fast easily formed at solvothermal temperature as low as 140 °C. Growth mechanism and magnetic properties of these Fe_3O_4 microflowers were also investigated.

2. Experimental section

2.1. Synthesis

All reagents are analytically pure and used as-received without further purification. In a typical procedure, $FeCl_3 \cdot 6H_2O$ (0.27 g) was dissolved into ethylene glycol (EG, 50 mL) to form a stable

*Corresponding author. Tel.: +86 516 83885096; fax: +86 516 83591054.
E-mail address: ronglijcumt@163.com (R. Jiang).

0272-8842/$ - see front matter © 2013 Elsevier Ltd and Techna Group S.r.l. All rights reserved.
http://dx.doi.org/10.1016/j.ceramint.2013.09.025

orange solution. Then, a reverse microemulsion solution was prepared by adding 0.6 mL of 0.05 M KOH aqueous solution into OP/cyclohexane/*n*-octanol system (according to the mass ratio OP/cyclohexane/*n*-octanol = 5/16/4), the mixing solution was stirred for 10 min until it became transparent. Subsequently, 0.6 mL of the above stable orange solution was added dropwise into the microemulsion and kept under stirring for another 30 min. Afterwards, the resulting solution was transferred to a 30-mL Teflon-lined stainless-steel autoclave and maintained at 140 °C for 10 h. After cooling to the room temperature naturally, black precipitates were collected by centrifugation, and washed with deionized water and absolute ethanol repeatedly and dried in vacuum at 50 °C for 4 h.

2.2. Characterization

Phase identification was done by the powder X-ray diffraction (XRD) using an X-ray diffractometer (the Philips X'Pert) with Cu Kα radiation ($\lambda = 1.5406$ Å). Field emission scanning electron microscopy (FE-SEM) images and X-ray energy dispersive spectroscopy (EDS) analyses were obtained using a Sirion 200 FEG microscope, and the as-synthesized products were dispersed on the Si substrate. Transmission electron microscopy (TEM) and selected area electron diffraction (SAED) observations were carried out on a JEM-200CX instrument (operated at 200 kV). The magnetic hysteresis loops were measured by a vibrating sample magnetometer (VSM, Lake Shore 7410).

3. Results and discussion

Fig. 1(a) and (b) displays the FE-SEM images of the as-prepared products, which depict that the products are well-grown flower-like structures with diameter of ~5 μm. The assembly of flower-like microstructures consisted of tens of hundreds of nanosheets, whose surface is rough with the thickness of ~25 nm. Fig. 1(c) presents the TEM image of an individual nanosheet, from which we can see that the nanosheet is made up of numerous small nanoparticles whose size is about 10 nm. The SAED rings (Fig. 1(d)), taken from the microflower, exhibit the high polycrystalline nature of the product. Fig. 2(a) describes XRD patterns of the flower-like microstructures. All detectable peaks can be assigned to a pure cubic structured Fe_3O_4 (JCPDS no. 65-3107). The EDS data (Fig. 2(b)) have also been recorded with the microflower, where signals from Fe, O and Si were detected, among which Si comes from the substrate, Fe and O come from the product. It can further confirm the Fe_3O_4 compositions of the sample.

For better understanding the formation mechanism of the flower-like microstructures, reaction products prepared at different growth times were examined by XRD and FE-SEM observations. Fig. 3 lists representative XRD patterns of the samples generated at selected intervals, the results depict that all the peaks can be indexed to cubic structure of magnetite according to JCPDS card no. 65-3107. Noticeably, the intensities of the peaks are gradually increased with increasing the reaction time, suggesting that the longer reaction time favors the crystallization of Fe_3O_4 phase. Fig. 4 plots the FE-SEM images

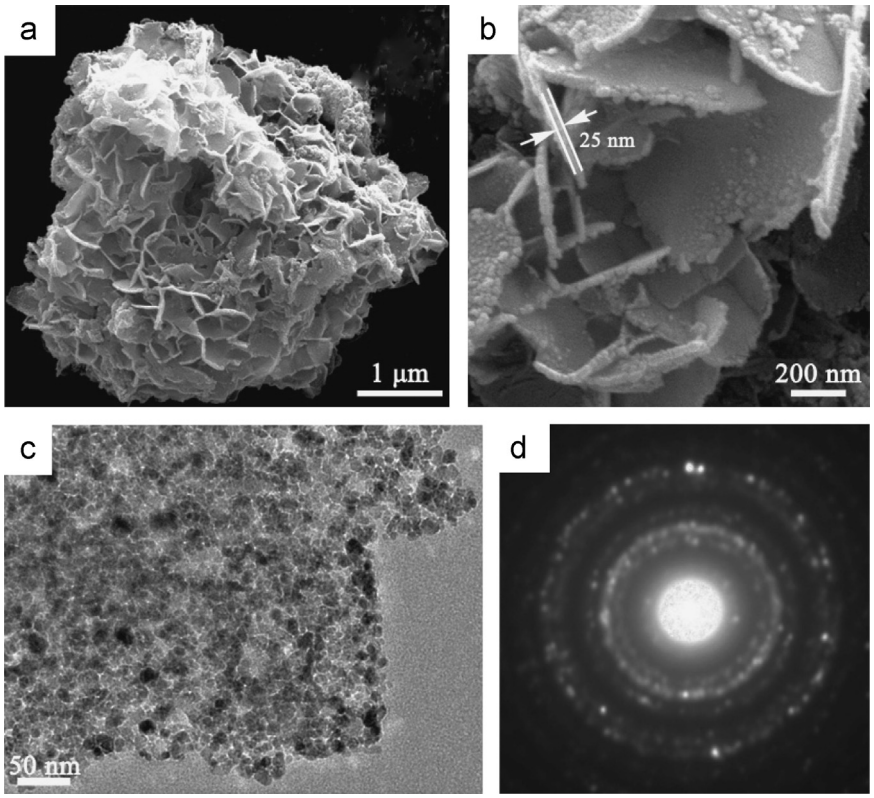

Fig. 1. FE-SEM images (a, b), TEM image (c) and SAED pattern (d) of the flower-like magnetite synthesized at 140 °C for 10 h.

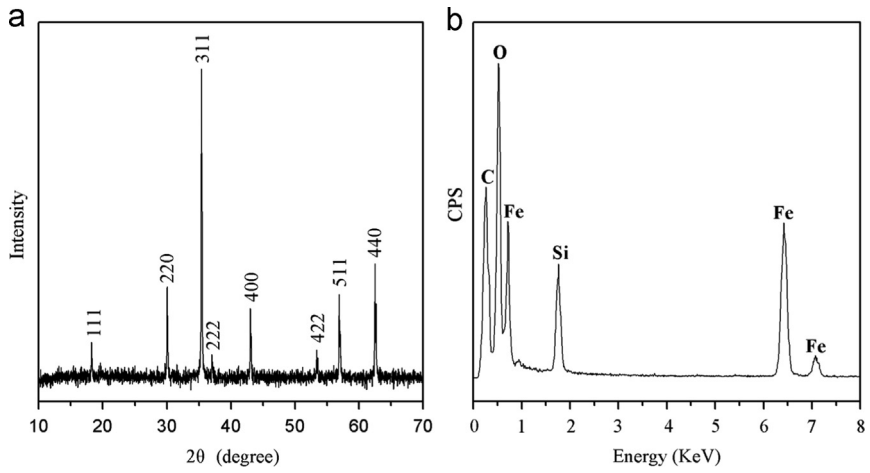

Fig. 2. XRD pattern (a) and EDS data (b) of the flower-like magnetite obtained at 140 °C for 10 h.

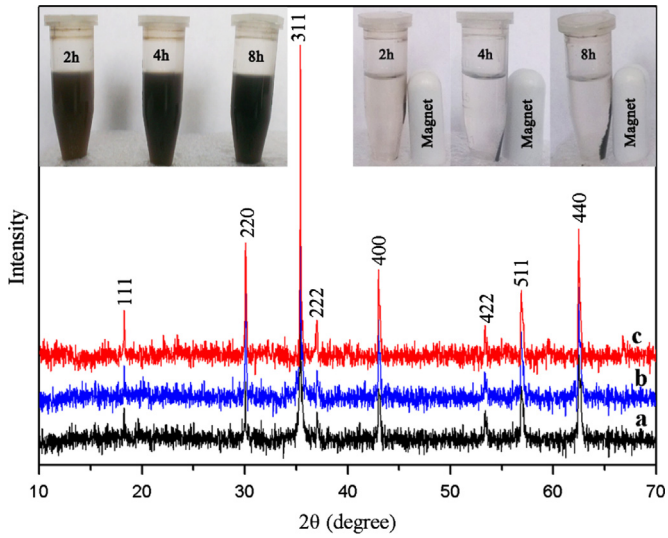

Fig. 3. XRD patterns of magnetite samples at different stages: (a) 2 h, (b) 4 h and (c) 8 h. The inset photographs show that the as-synthesized magnetite sample can be easily dispersed in absolute ethanol and also be drawn from the solution to the sidewall of the vial by an assistant magnet field.

of the same samples as listed in Fig. 3. At the early stage, the nanoparticles with diameter of ~30 nm were formed when dropping the stable orange $FeCl_3$ ethylene glycol solution into the KOH microemulsion and the subsequent solvothermal treatment at 140 °C for 2 h, as a result of the homogeneous nucleation and crystallization in the system (Fig. 4(a)). As the reaction time was prolonged to 4 h, some nanosheets began to appear in the restricted water pools with the help of the nanoparticles, as marked by white rings (Fig. 4(b)). When the reaction proceeded to 8 h, more nanosheets developed (Fig. 4(c)). This observation is based on the oriented growth habit of Fe_3O_4 crystals and the selective absorption of surfactant molecules on the faces of the prime crystals [22–24]. After the formation of nanosheets, the main nanobuilding blocks of microflowers has been built. While the aging time was extended to 10 h, the perfectly flower-like microstructures fully received as a consequence of the self-assembly process (see Fig. 1(a)). On the basis of shape evolution discussed above, we believe that the preparation of flower-like Fe_3O_4 experienced a nanobuilding blocks self-assembly process on account of the oriented growth behavior of Fe_3O_4 crystals. The schematic diagram of the proposed growth mechanism of Fe_3O_4 microflowers is shown in Fig. 5.

The magnetic properties of the well-defined Fe_3O_4 microflowers were measured at 300 K using VSM from −20,000 to 20,000 Oe. Fig. 6 shows the hysteresis loops of the flower-like Fe_3O_4 microstructures. The result indicates that the reversible characteristic with no hysteresis, illustrating that the sample is superparamagnetic at room temperature. Generally, magnetite particles with sizes below 30 nm can have superparamagnetic properties [25]. The size of flower-like Fe_3O_4 is more than 1 μm, but they still exhibit superparamagnetic behavior, which can be attributed to the fact that the flowers are assembled by nanosheets, while the nanosheets are composed of primary nanoparticles about 10 nm, less than the critical value 30 nm. Superparamagnetic magnetite nanoparticles always have low saturation magnetization because of their small size [26]. But, our superparamagnetic Fe_3O_4 microflowers show relative high saturation magnetization (69.1 emu/g), which possibly for their self-assembly structure and small amount of nanoparticles existing in the sample [23,27,28]. More detailed investigations on the magnetic properties and the factors influencing formation of this sample are in progress.

4. Conclusions

In summary, flower-like Fe_3O_4 microstructures have been successfully synthesized by a facile single-microemulsion-based solvothermal route. The growth mechanism of the as-made Fe_3O_4 microflowers was proposed, which includes the formation of nanoparticles and their oriented growth as well as the self-assembly process. The magnetism analysis elucidates that the as-grown sample is superparamagnetic with a saturation magnetization of 69.1 emu/g. It is expected that these flower-like structures will offer more opportunities for both fundamental research and a crucial object for building blocks

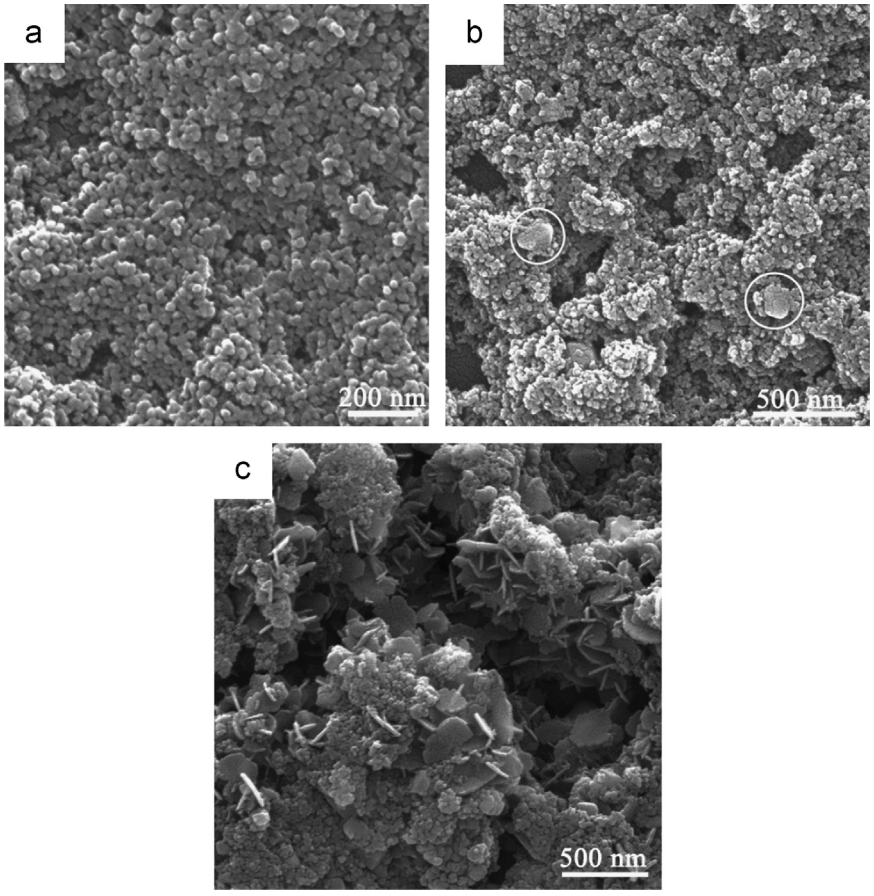

Fig. 4. FE-SEM images of magnetite products at different times: (a) 2 h, (b) 4 h and (c) 8 h.

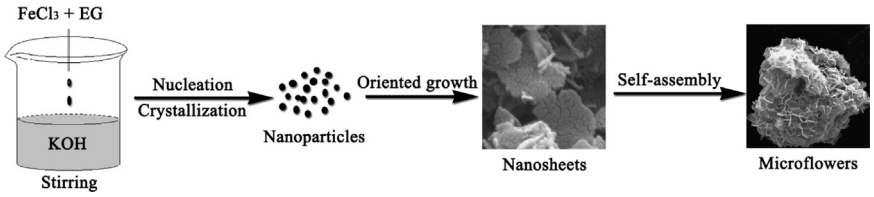

Fig. 5. Schematic illustration of the morphological evolution process of magnetite microflowers.

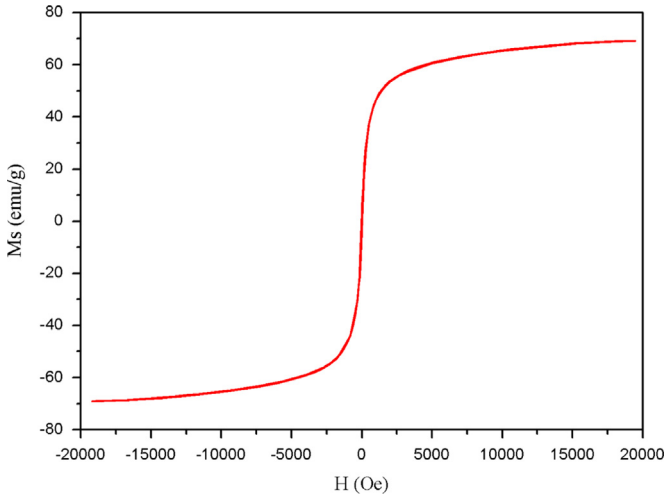

Fig. 6. Magnetic hysteresis loops of magnetite microflowers at room temperature.

for nanodevices in the future. Additionally, the present work may open a novel convenient and effective way to prepare other metal oxide hierarchical structured micro/nanomaterials.

Acknowledgments

This work was supported by the Specialized Research Fund for the Doctoral Program of Higher Education of China (20100095110009) and the Fundamental Research Funds for the Central Universities (2010LKHX05, 2012LWA05).

References

[1] P. Tartaj, M.P. Morales, T. Gonzalez-Carreño, S. Veintemillas-Verdaguer, C.J. Serna, The iron oxides strike back: from biomedical applications to energy storage devices and photoelectrochemical water splitting, Advanced Materials 23 (2011) 5243–5249.

[2] C.T. Yavuz, J.T. Mayo, W.W. Yu, A. Prakash, J.C. Falkner, S. Yean, L. Cong, H.J. Shipley, A. Kan, M. Tomson, D. Natelson, V.L. Colvin,

Low-field magnetic separation of monodisperse Fe_3O_4 nanocrystals, Science 314 (2006) 964–967.
[3] D.H. Han, J.P. Wang, H.L. Luo, Crystallite size effect on saturation magnetization of fine ferrimagnetic particles, Journal of Magnetism and Magnetic Materials 136 (1994) 176–182.
[4] F. Caruso, M. Spasova, A. Susha, M. Giersig, R.A. Caruso, Magnetic nanocomposite particles and hollow spheres constructed by a sequential layering approach, Chemistry of Materials 13 (2001) 109–116.
[5] T. Hyeon, S.S. Lee, J. Park, Y. Chung, H.B. Na, Synthesis of highly crystalline and monodisperse maghemite nanocrystallites without a size-selection process, Journal of the American Chemical Society 123 (2001) 12798–12801.
[6] Y. Deng, Q. Di, C. Deng, X. Zhang, D. Zhao, Superparamagnetic high-magnetization microspheres with an Fe_3O_4@SiO_2 core and perpendicularly aligned mesoporous SiO_2 shell for removal of microcystins, Journal of the American Chemical Society 130 (2008) 28–29.
[7] X.W. Liu, Q.Y. Hu, Z. Fang, Q. Wu, Q.B. Xi, Carboxyl enriched monodisperse porous Fe_3O_4 nanoparticles with extraordinary sustained-release property, Langmuir 25 (2009) 7244–7248.
[8] H. Deng, X.L. Li, Q. Peng, X. Wang, J.P. Chen, Y.D. Li, Monodisperse magnetic single-crystal ferrite microspheres, Angewandte Chemie International Edition 44 (2005) 2782–2785.
[9] L. Vayssieres, C. Sathe, S.M. Butorin, D.K. Shuh, J. Nordgren, J.H. Guo, One-dimensional quantum-confinement effect in α-Fe_2O_3 ultrafine nanorod arrays, Advanced Materials 17 (2005) 2320–2323.
[10] J.X. Wan, X.Y. Chen, Z.H. Wang, X.G. Yang, Y.T. Qian, A soft-template-assisted hydrothermal approach to single-crystal Fe_3O_4 nanorods, Journal of Crystal Growth 276 (2005) 571–576.
[11] X.G. Wen, S.H. Wang, Y. Ding, Z.L. Wang, S.H. Yang, Controlled growth of large-area, uniform, vertically aligned arrays of alpha-Fe_2O_3 nanobelts and nanowires, The Journal of Physical Chemistry B 109 (2005) 215–220.
[12] C.J. Jia, L.D. Sun, Z.G. Yan, L.P. You, F. Luo, X.D. Han, Y.C. Pang, Z. Zhang, C.H. Yan, Single-crystalline iron oxide nanotubes, Angewandte Chemie International Edition 44 (2005) 4328–4333.
[13] L.L. Li, Y. Chu, Y. Liu, D. Wang, Solution-phase synthesis of single-crystalline Fe_3O_4 magnetic nanobelts, Journal of Alloys and Compounds 472 (2009) 271–275.
[14] S. Singamaneni, V.N. Bliznyuk, C. Binek, E.Y. Tsymbal, Magnetic nanoparticles: recent advances in synthesis, self-assembly and applications, Journal of Materials Chemistry 21 (2011) 16819–16845.
[15] N.N. Guan, D.J. Sun, J. Xu, Self-assembly of iron oxide nanoparticles into oriented nanosheets by one-pot template-free synthesis at low pH, Materials Letters 63 (2009) 1272–1274.
[16] G.B. Sun, B.X. Dong, M.H. Cao, B.Q. Wei, C.W. Hu, Hierarchical dendrite-like magnetic materials of Fe_3O_4, γ-Fe_2O_3, and Fe with high performance of microwave absorption, Chemistry of Materials 23 (2011) 1587–1593.
[17] Z.C. Guo, C.L. Shao, M.Y. Zhang, J.B. Mu, Z.Y. Zhang, P. Zhang, B. Chen, Y.C. Liu, Dandelion-like Fe_3O_4@CuTNPc hierarchical nanostructures as a magnetically separable visible-light photocatalyst, Journal of Materials Chemistry 21 (2011) 12083–12088.
[18] M. Basu, A.K. Sinha, S. Sarar, M. Pradhan, S.M. Yusuf, Y. Negishi, T. Pal, Hierarchical superparamagnetic magnetite nanowafers from a resin-bound $[Fe(bpy)_3]^{2+}$ matrix, Langmuir 26 (2010) 5836–5842.
[19] L.S. Zhong, J.S. Hu, H.P. Liang, A.M. Cao, W.G. Song, L.J. Wan, Self-assembled 3D flowerlike iron oxide nanostructures and their application in water treatment, Advanced Materials 18 (2006) 2426–2431.
[20] Z.H. Ai, K.J. Deng, Q.F. Wan, L.Z. Zhang, S.C. Lee, Facile microwave-assisted synthesis and magnetic and gas sensing properties of Fe_3O_4 nanoroses, The Journal of Physical Chemistry C 114 (2010) 6237–6242.
[21] X.Y. Li, Z.J. Si, Y.Q. Lei, X.N. Li, J.K. Tang, S.Y. Song, H.J. Zhang, Hierarchically structured Fe_3O_4 microspheres: morphology control and their application in wastewater treatment, CrystEngComm 13 (2011) 642–648.
[22] Y.W. Jun, J.H. Lee, J.S. Choi, J. Cheon, Symmetry-controlled colloidal nanocrystals: nonhydrolytic chemical synthesis and shape determining parameters, The Journal of Physical Chemistry B 109 (2005) 14795–14806.
[23] J. Lu, X.L. Jiao, D.R. Chen, L. Wei, Solvothermal synthesis and characterization of Fe_3O_4 and γ-Fe_2O_3 nanoplates, The Journal of Physical Chemistry C 113 (2009) 4012–4017.
[24] X.M. Liu, J.K. Kim, Solvothermal synthesis and magnetic properties of magnetite nanoplatelets, Materials Letters 63 (2009) 428–430.
[25] J. Lee, T. Isobe, M. Senna, Preparation of ultrafine Fe_3O_4 particles by precipitation in the presence of PVA at high pH, Journal of Colloid and Interface Science 177 (1996) 490–494.
[26] C. Hui, C.M. Shen, T.Z. Yang, L.H. Bao, J.F. Tian, H. Ding, C. Li, H.J. Gao, Large-scale Fe_3O_4 nanoparticles soluble in water synthesized by a facile method, The Journal of Physical Chemistry C 112 (2008) 11336–11339.
[27] Y. Wang, Q.S. Zhu, H.G. Zhang, Fabrication and magnetic properties of hierarchical porous hollow nickel microspheres, Journal of Materials Chemistry 16 (2006) 1212–1214.
[28] L.J. Zhao, H.J. Zhang, Y. Xing, S.Y. Song, S.Y. Yu, W.D. Shi, X.M. Guo, J.H. Yang, Y.Q. Lei, F. Cao, Morphology-controlled synthesis of magnetites with nanoporous structures and excellent magnetic properties, Chemistry of Materials 20 (2008) 198–204.